New Products and Data for Better Monitoring of Arctic Black Carbon

ABC-iCAP Project
Technical Report 3

New Products and Data for Better Monitoring of Arctic Black Carbon

ABC-iCAP Project
Technical Report 3

New Products and Data for Better Monitoring of Arctic Black Carbon
ABC-iCAP Project Technical Report 3

Citation
Asmi, E., S. Eckhardt, N. Evangeliou, K. Luoma, A. Hyvärinen, 2023. New Products and Data for Better Monitoring of Arctic Black Carbon. Arctic Black Carbon impacting on Climate and Air Pollution (ABC-iCAP) Project Technical Report 3. December 2023 iii+17pp.

Authors
Eija Asmi[1], Sabine Eckhardt[2], Nikolaos Evangeliou[2], Krista Luoma[1], Antti Hyvärinen[1]

Affiliations
[1]Finnish Meterological Institute (FMI)
[2]Norwegian Institute for Air Research (NILU)

Acknowledgment
The authors would like to thank all other colleagues who contributed to the production and review of this report.

Layout and technical production
Burnthebook, United Kingdom (www.burnthebook.co.uk)

This project is funded by the European Union

The report was prepared as one of the deliverables under the project *Arctic Black Carbon impacting on Climate and Air Pollution (ABC-iCAP)*, funded by the European Union.

abc-icap.amap.no

Contents

Summary

A detailed analysis where BC concentrations measured at the Pallas, northern Finland and Baranova, Arctic Russia station was combined with transport modelling has been performed. The ECLIPSE inventory and GFED biomass burning emissions have been used to obtain source specific BC concentrations at the receptor. Overall, the levels of the observed and measured BC match very well at Pallas and are slightly underestimated at Baranova (Tab. 1). The latter could be explained by the underestimated emission source contributions from Siberia, as has been suggested in earlier studies.

There is, however, seasonal variability. At Pallas during summertime the BC concentration is overestimated, while in wintertime it is underestimated by the model. Our analysis shows that the most important sources for BC in Pallas are biomass burning, domestic heating, transport, and industry. BC from biomass burning is only occurring in summer, while domestic heating gets an important share during wintertime.

At Pallas pollution with a high fraction of domestic burning contribution is overestimated by the model, while events with dominated biomass burning contribution is underestimated.

Table 1. Average observed and modelled BC concentration in Pallas and Baranova during period 2019-2020.

	Observed	Modelled
Pallas	44 ng/m^3	45 ng/m^3
Baranova	54 ng/m^3	48 ng/m^3

Background

1

To accurately predict the future climate of the Arctic, a comprehensive understanding of Arctic black carbon (BC) concentrations and their sources is essential. Transport modeling serves as an effective tool for the spatial estimation of the impact of various sources, such as flaring, biomass burning, energy production, and traffic, along with their seasonal variations. However, for these estimates to be trustworthy, the models require validation and refinement through actual measurement data. Presently, there are very few long-term BC datasets available from the Arctic region (EU-funded Action on Black Carbon in the Arctic, 2019).

At the ABC-iCAP workshop, held at the Pallas station in Finnish Lapland, a key observation was made: "Pallas stands out in the modeling of Arctic BC concentrations, as indicated by results from both Sabine (FLEXPART) and Naga (MRI-ESM2). These models tend to overestimate surface BC concentration, and the underlying reasons for this discrepancy remain unclear."

A pivotal topic of discussion at the workshop revolved around the varying definitions of BC. It was noted that BC mass, Elemental Carbon (EC) mass, and BC absorption represent distinct metrics, and a range of techniques should be concurrently evaluated and applied in atmospheric monitoring. This multi-faceted approach is necessary to meet the diverse needs of the scientific community.

This report aims to address these concerns by presenting model-derived, source-specific BC mass concentration data for three Arctic measurement stations: Pallas and Baranova. It delves into the relative importance of different BC sources, as well as their seasonal and spatial variations in the Arctic. The report also compares novel BC data collected at these stations with model predictions, discussing any observed discrepancies and their possible drivers.

The Finnish Meteorological Institute's Pallas research station

BC sources at Arctic stations calculated by FLEXPART

2

For investigating in the source regions of the BC measured at the stations, we used the Lagrangian transport model FLEXPART (Pisso et al., 2019). In previous studies it has been shown that it can model well the BC conenctration close to sources (Evangeliou et al., 2018), but also in the Arctic (Eckhardt et al., 2015). FLEXPART simulates the source-receptor relationship for aerosol tracer arriving at the 3 stations of interest. The aerosol tracer which experiences scavenging (Grythe et al., 2017) is kept in the model for 30 days. FLEXPART simulates advection by mean wind, turbulent processes and convection based on input data from the ECMWF reanalysis project ERA-5. The windfields are available hourly on a 0.5 degree resolution, spanning over 138 levels, capturing the whole atmospheric column up to 40km. The transport simulations where then combined with BC emissions obtained from ECLIPSEv6 (Klimont et al., 2017). The emissions are seperated for different source categories: DOM BC: Modelled contribution to surface black carbon (BC) from residential and commercial sector plotted on a map (three projections). DOM includes emissions from combustion in heating and cooking stoves and boilers in households and public and commercial buildings (Klimont et al., 2017).

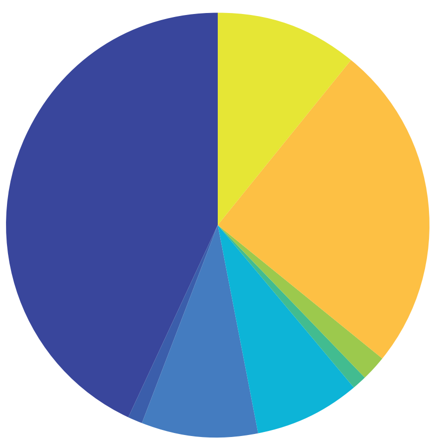

Figure 1. Modelled relative contibution of BC source categories for the Pallas station during the years 2019-2020, based on FLEXPART simulations.

- **ENE BC:** Modelled contribution to surface black carbon (BC) from energy production sector plotted on a map (three projections). ENE includes emissions from combustion processes in power plants and generators (ECLIPSEv6, Klimont et al., https://doi.org/10.5194/acp-17-8681-2017).
- **IND BC:** Modelled contribution to surface black carbon (BC) from industrial combustion plotted on a map (three projections). IND includes emissions from industrial boilers and industrial production processes (ECLIPSEv6, Klimont et al., https://doi.org/10.5194/acp-17-8681-2017).
- **FLR BC:** Modelled contribution to surface black carbon (BC) from gas flaring plotted on a map (three projections). FLR includes emissions from oil and gas facilities (ECLIPSEv6, Klimont et al., https://doi.org/10.5194/acp-17-8681-2017).
- **SHP BC:** Modelled contribution to surface black carbon (BC) from shipping activities in in-land waters plotted on a map (three projections) (ECLIPSEv6, Klimont et al., https://doi.org/10.5194/acp-17-8681-2017).
- **WST BC:** Modelled contribution to surface black carbon (BC) from waste treatment and disposal sector plotted on a map (three projections). WST resembles emissions from waste incineration and treatment (ECLIPSEv6, Klimont et al., https://doi.org/10.5194/acp-17-8681-2017).
- **TRA BC:** Modelled contribution to surface black carbon (BC) from transportation sector plotted on a map (three projections). TRA includes emissions from all land-based transport of goods, animals and persons on road networks and off-road activities (ECLIPSEv6, Klimont et al., https://doi.org/10.5194/acp-17-8681-2017).
- **Fire BC:** Modelled contribution to surface black carbon (BC) from open biomass burning (excluding agricultural fires) plotted on a map (three projections) (GFEDv4, Giglio et al., https://doi.org/10.1002/jgrg.20042).

Figure 1 shows the importance of the different BC emission sources for the Pallas station. The domestic burning contribution is, with 43%, the most important one all over the year, and during wintertime the domestic sector counts for even 50%. The transport sector is the second most important one with 25%, followed by biomass burning, flaring and industry.

Model-measurement inter-comparison at Pallas

3

BC concentrations at Pallas have been measured since year 2005 (Hyvärinen et al., 2011). The BC data from Pallas is open, the concentration levels have been extensively compared with the other Arctic monitoring stations (e.g. Schmale et al., 2022) and with model results (e.g. Eckhardt et al., 2015). Currently, several advanced techniques are used simultaneously in Pallas to obtain reliable BC mass and aerosol absorption concentrations (Asmi et al., 2021).

During the concurrent measurements in years 2019 and 2020, the overall average BC mass concentration at Pallas was 44 ng / m3, in comparison to the modeled 45 ng /m3. Despite the overall good agreement, there are some evident discrepancies observed at day-to-day intercomparison (Fig 2).

Our conclusions from the model-measurement inter-comparison for Pallas at 3h time resolution are:

- Model tends to overestimate BC when station is inside the cloud or when main source is domestic burning during wintertime, when an inversion situation is present. The aerosol measured at the Pallas station has an average age of <11 days in winter.
- Model tends to underestimate BC in particular during summertime biomass burning events. In contrary to winter, the BC in Pallas in summer is more aged with an average age of about 14 days.

Data and model are not intercomparable during "cloud events", i.e. when the station is inside a cloud (see Fig. 2). For this reason, these data are not used in further analysis, yet a similar effect of over/underestimation is still observed (Fig. 3).

The next question is, if the observed occasional discrepancies between model and observations are derived

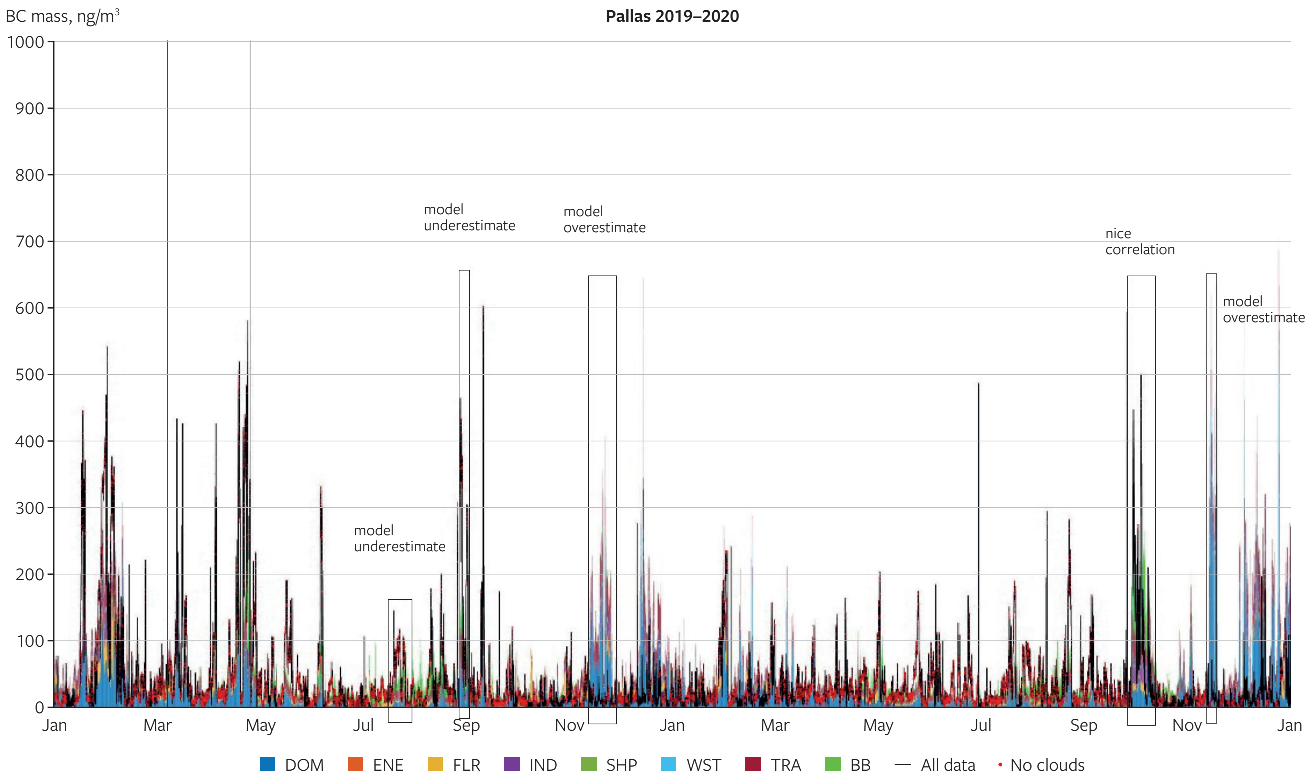

Figure 2. Modeled BC concentration from different source contributions (colors) and measured BC concentration, black line (all data) and red dots (only data with no clouds at site) at Pallas site.

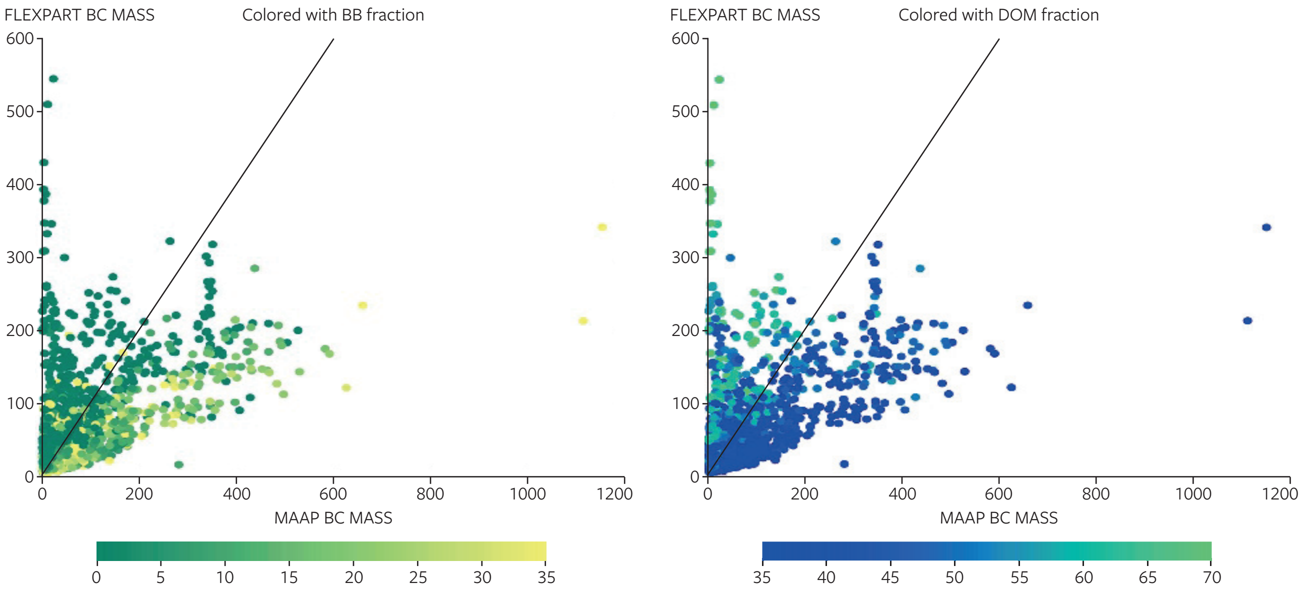

Figure 3. Modeled BC concentrations [ng / m3] (y-axis) as a function of measured BC concentration [ng / m3] (x-axis), for different BB (left) and DOM (right) mass source contribution fractions and 1:1 line for Pallas. Periods when station was inside a cloud are omitted from this intercomparison.

from the source characteristic emissions, aerosol processing during transport or BC aerosol physical properties, such as the aerosol age. Aging has a drastic impact on the BC aerosol light-absorption and could therefore impact on the measured mass concentration. The dependence of model-to-measurement ratio on air mass modelled average age, however, does not present a clear correlation (Fig 4).

The biomass burning aerosol in Pallas is more aged than other types of BC aerosol. When BB contribution to BC is >70%, the average age of the BC is >17days (Fig 4a). Model-to-measured BC additionally has a distinct dependency on measured BC concentration (Fig 4b). The model seems to underestimate the BC particularly at higher concentrations, vice versa, overestimate when BC concentration is low.

We analyzed the model-to-measured BC ratio and its' dependence on the BC concentration further by separating different source contributions and seasons with colors in Figure 5. Based on this, the impact of the source or the season is minor in comparison to the impact of the concentration, which remains as the determinant factor for the model-measurement discrepancy.

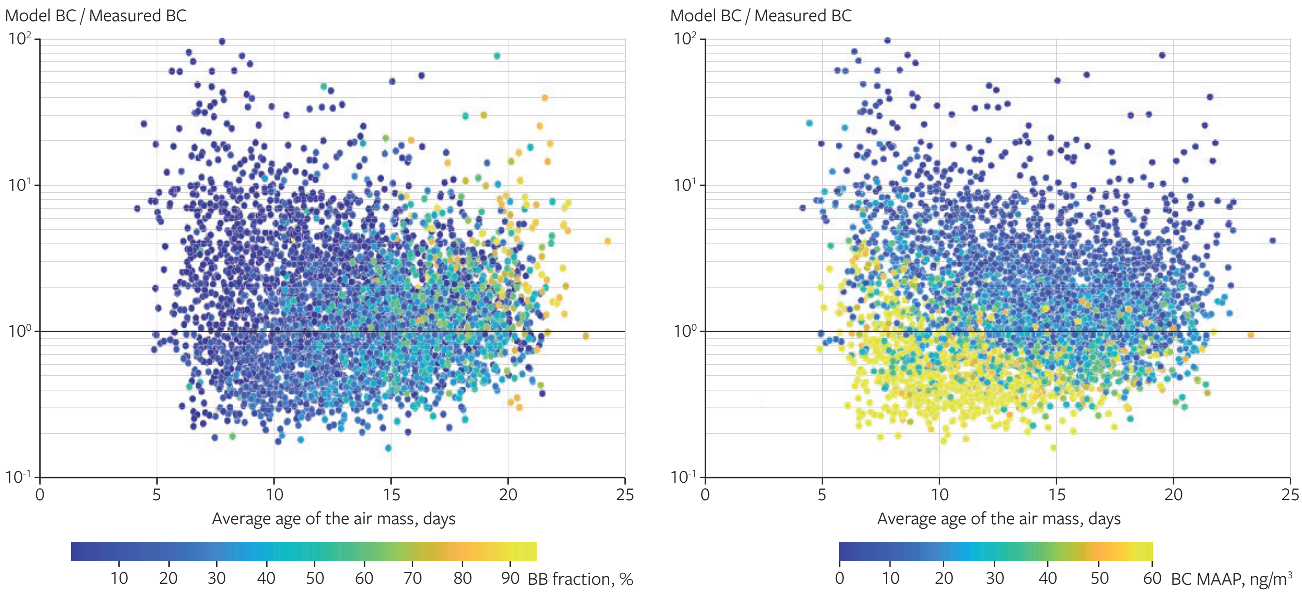

Figure 4. Ratio of model-to-measured BC (y-axis) as a function of air mass age (x-axis), colored with a) BB fraction and b) measured BC concentration for Pallas.

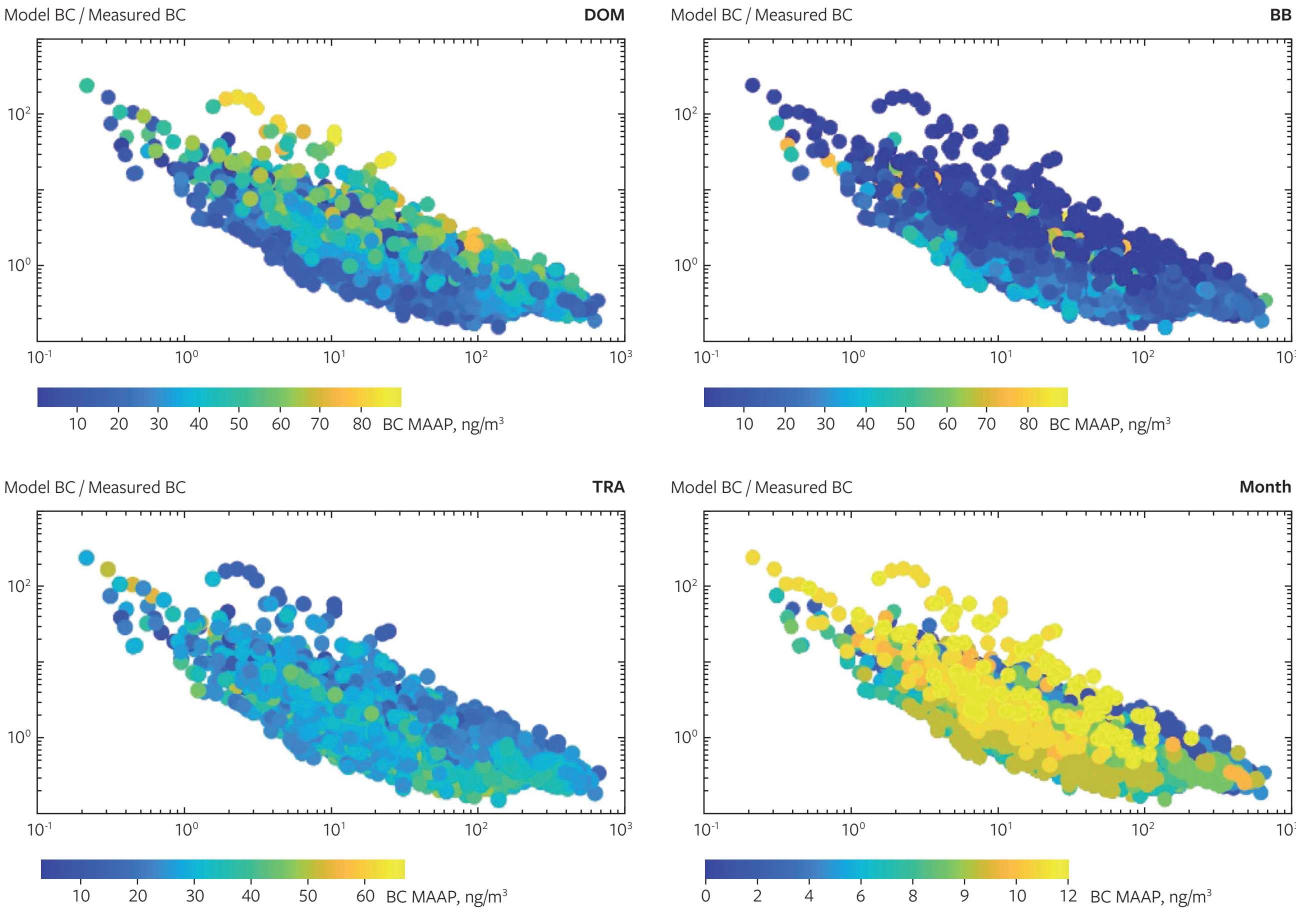

Figure 5. Ratio of model-to-measured BC (y-axis) as a function of measured BC mass, colored with emission % from a) domestic burning, b) biomass burning, c) traffic and d) month, at Pallas.

Case studies in Pallas

4

To get further insight on the model-measurement comparability during different types of BC transport episodes, two very different cases from Pallas were selected for a closer examination. First, in summer 2019, when measured BC concentration was about twice as high as modelled (Fig. 6). The main sources based on model were domestic burning, traffic and biomass burning. Second selected period was episode in winter 2019, when the measured BC concentration was only about 10% of the modelled (Fig. 7). The main sources based on model were domestic burning and traffic. Figure 8 shows the emission sensitivity maps for the two time periods. The emission source areas during both periods are in eastern and northern Europe, and over the Atlantic. Likely, the summer wildfires in Eastern Europe, and the cold trapping inversion in winter, have a major influence on the increasing BC levels in Pallas.

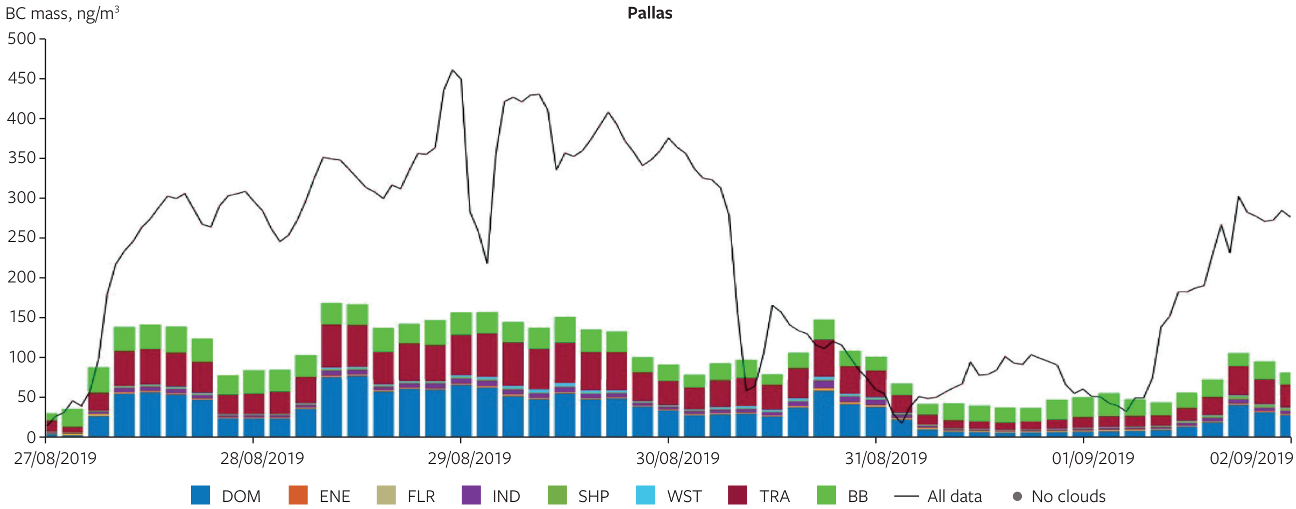

Figure 6. A week in the end of August, 2019 in Pallas when measured BC was clearly higher than modelled. BC sources were BB, DOM and TRA.

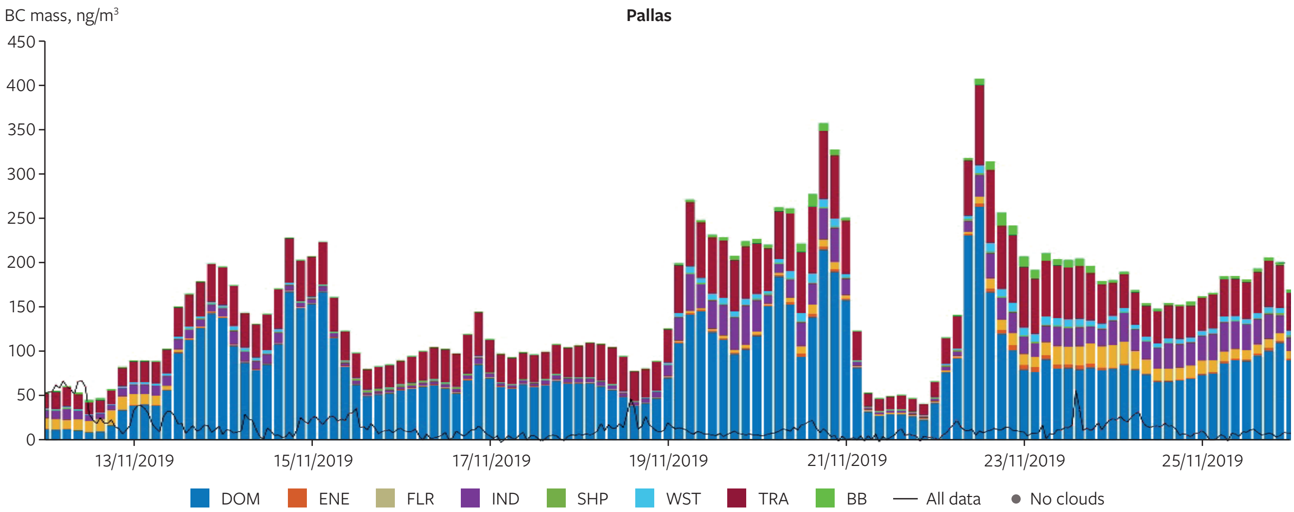

Figure 7. A two weeks period in the end of November 2019 in Pallas when measured BC was clearly lower than modelled. BC sources were DOM and TRA, also IND and FLR.

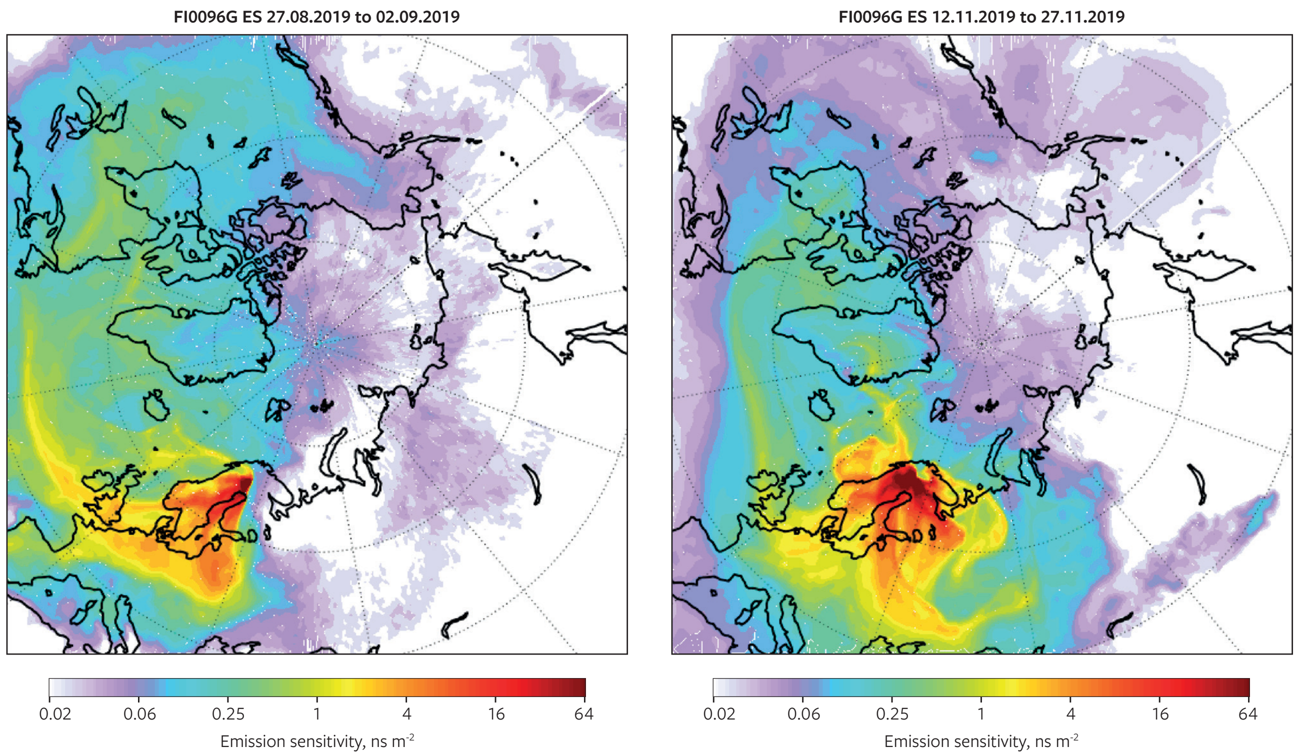

Figure 8: Emission sensitivities for the two time periods presented in Figs 6 and 7.

Model-measurement discrepancies at different stations

5

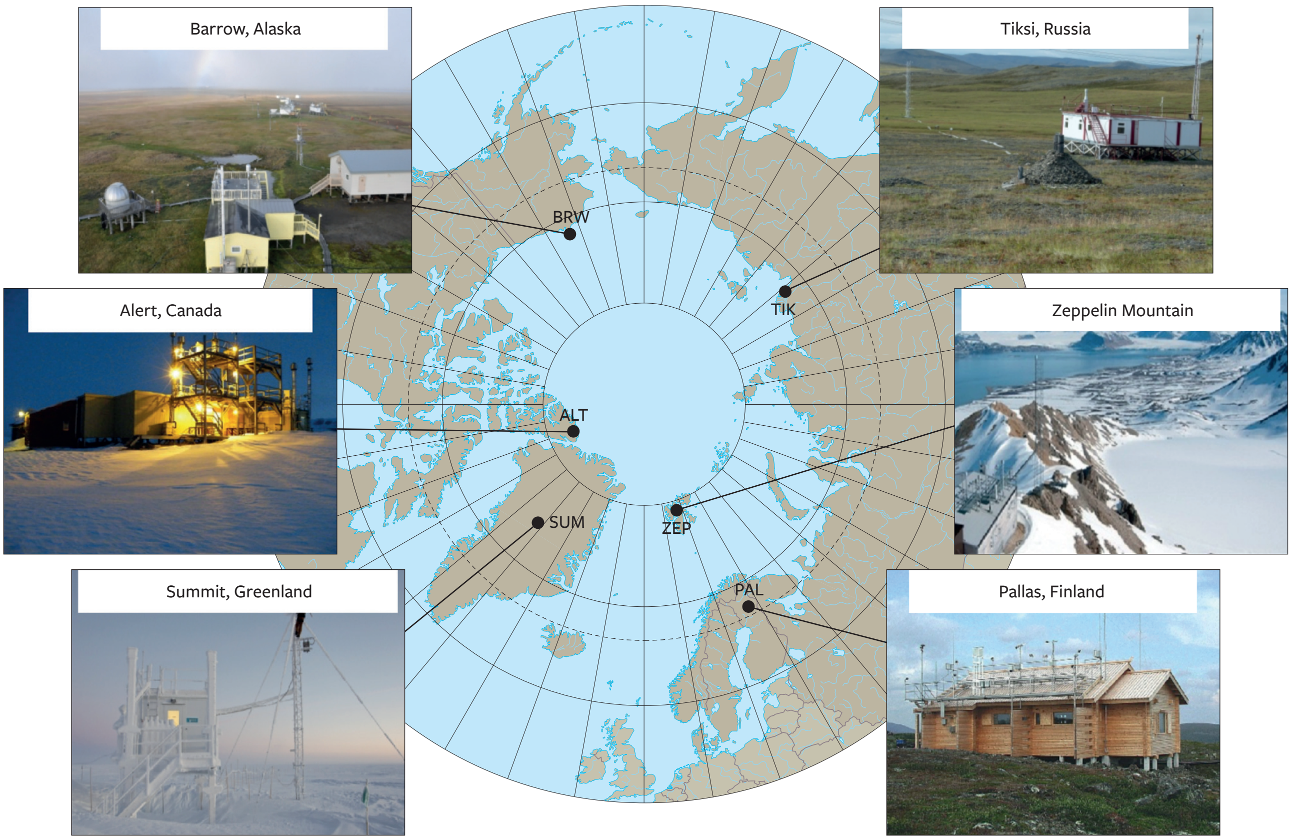

Figure 9. Location of station Cape Baranova is marked within the network of Arctic stations with a red star: Cape Baranova, Bolshevik island, North Land (N79°16.824', E101°37.053).

For this report, new BC data were obtained from a Baranova station, located in high-Arctic Russia (Fig 9).

According to the source inventories and FLEXPART, the main BC sources at Baranova are different from those at Pallas, where the highest relative contribution is flaring (40%), biomass burning (22%), and domestic combustion (16%) (Fig 10).

Again, good agreement between measurements and model was obtained (Fig 11). During the concurrent measurements in years 2019 and 2020, the overall average BC mass concentration at Baranova was 54 ng / m3, in comparison to the modeled 48 ng /m3. The minor difference might be explained by some unaccounted sources near Baranova, such as Siberian fires, as suggested earlier by Eckhardt et al., 2015.

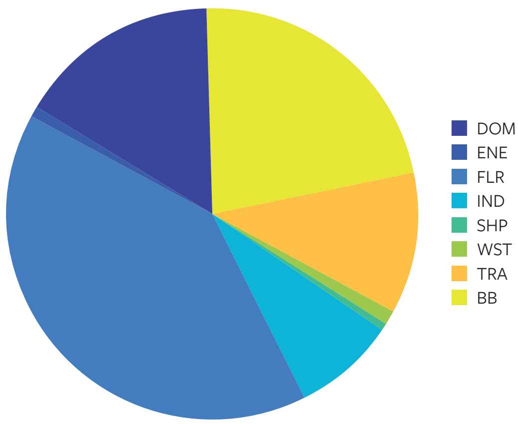

Figure 10. Modelled relative contribution of the different emission sources of BC in Baranova during years 2019-2020, based on FLEXPART.

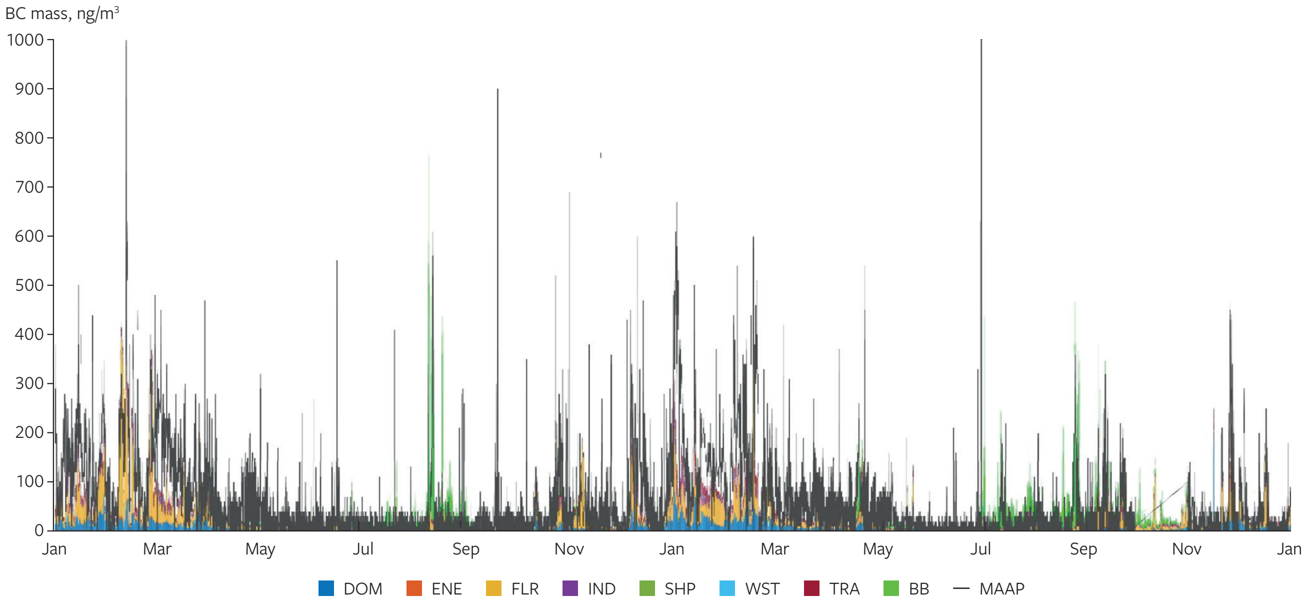

Figure 11. Modeled BC concentration from different source contributions (colors) and measured BC concentration (black line) at Baranova 2019-2020. In addition, we could conclude that in Baranova
• Wintertime BC concentrations are elevated due to flaring and domestic burning. Model and measurements coincide well here.
• Summertime concentrations occasionally elevated due to biomass burning.

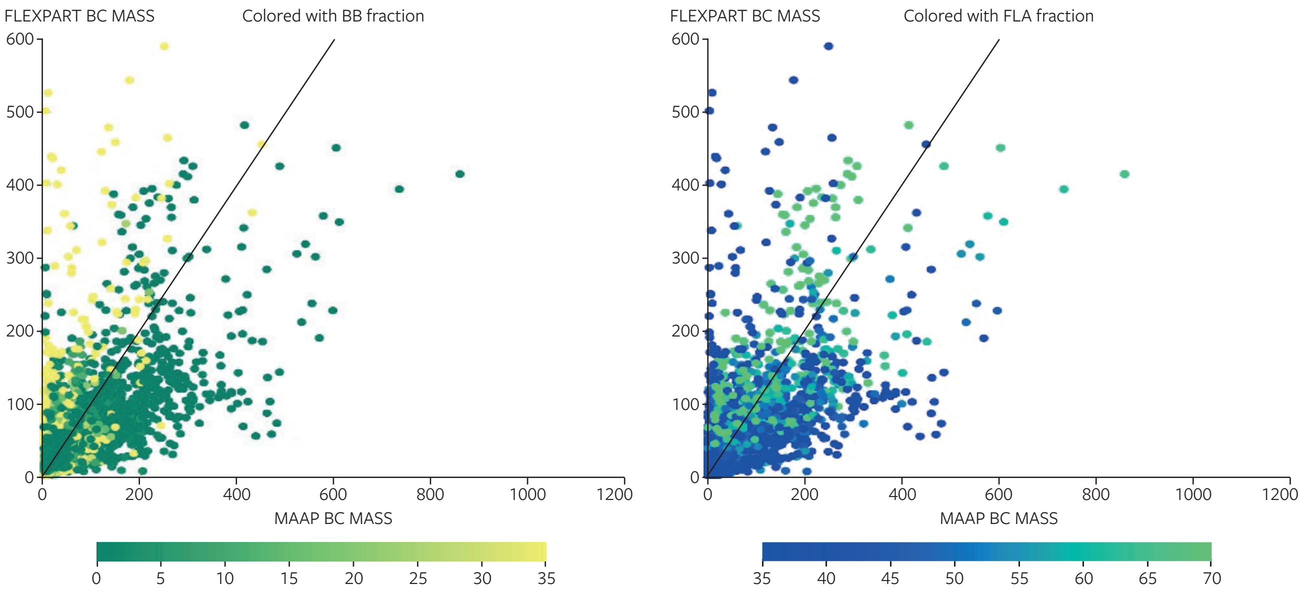

Figure 12. Modeled BC concentrations [ng / m3] (y-axis) as a function of measured BC concentration [ng / m3] (x-axis), for different BB (left) and FLA (right) mass source contribution fractions and 1:1 line for Baranova.

Biomass burning sources are closer to Baranova station than to Pallas and consequently, the model-to-measurement ratio is different in Baranova than in Pallas for BB aerosols. FLEXPART shows a higher BC source contribution from biomass burning than measurements actually detect (Fig 12a). For flaring model-to-measurement discrepancy is not as clear (Fig 12b).

In Baranova, contrary to Pallas, both flaring and biomass plumes can have various atmospheric ages (Fig 13). We performed an analysis for the model observation fit depending on the average age of the aerosol. The age is mainly between 2 and 12 days and as shown above this varies with the dominating source sector. Fig. 13 shows, that for short travel distances the model underestimates, while for longer travel distances, which corresponds to an higher age the model overestimates.

In Baranova, the BC concentration is clearly over the instrument detection limit (30 min value: < 20 ng/m³ BC) during winter haze season, when main sources are anthropogenic. Then the model tends to underestimate the surface BC concentration, similar to Pallas when concentration is high (Figs 14 and 15).

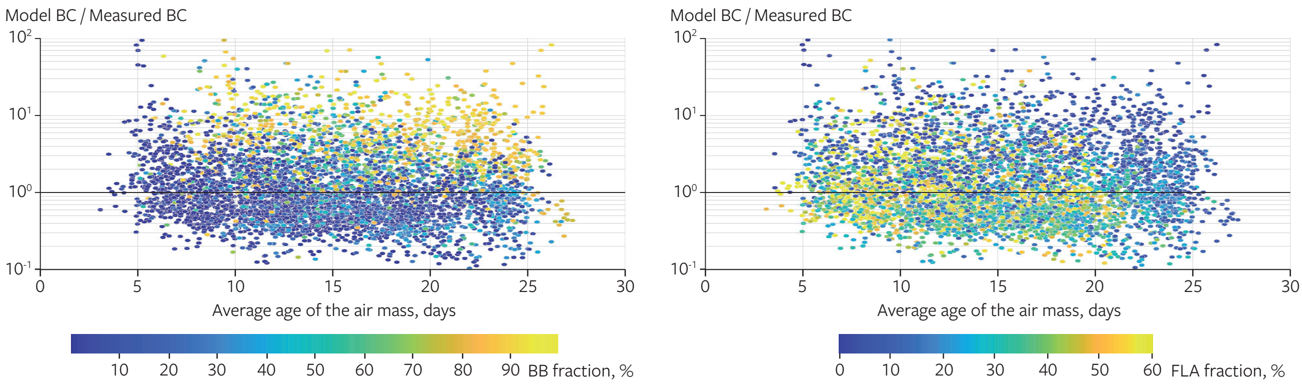

Figure 13. Ratio of model-to-measured BC (y-axis) as a function of air mass age (x-axis), colored with a) biomass burning (BB) fraction and b) flaring (FLA) fraction at Baranova during years 2019-2020.

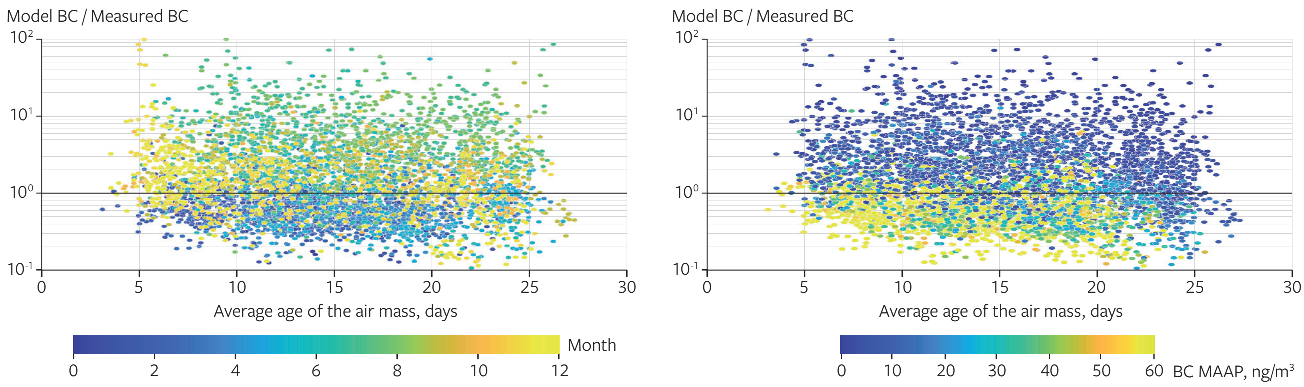

Figure 14. Ratio of model-to-measured BC as a function of air mass age (x-axis), colored with a) month of the year (color) and b) measured BC mass at Baranova 2019-2020.

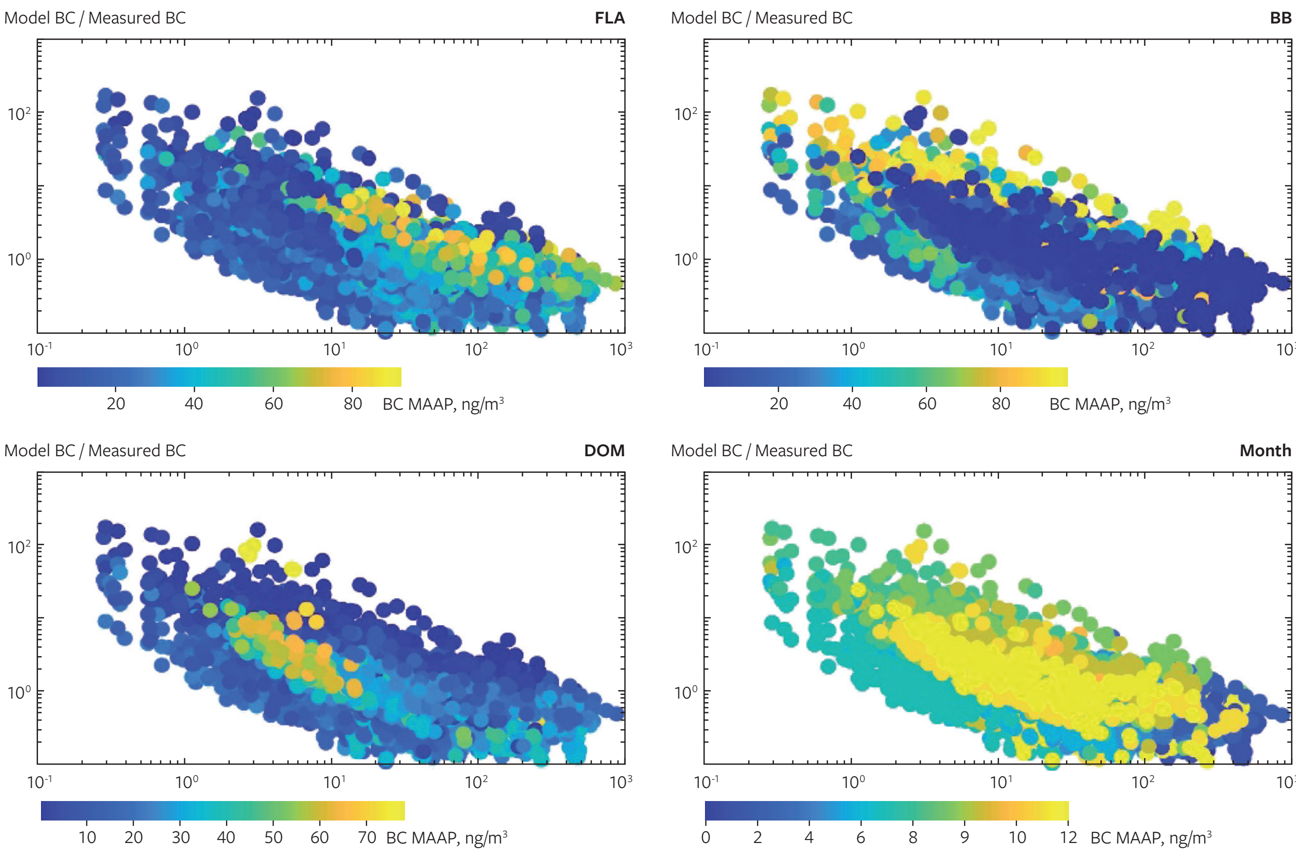

Figure 15. Ratio of model-to-measured BC as a function of measured BC mass, colored with emission % from a) flaring, b) biomass burning, c) domestic burning and d) month, at Baranova.

Conclusions

6

- BC sources and age vary with location in the Arctic
- Annual average BC concentrations are well captured by model.
- Median ratios Model-to-Measured BC were 1.33 (Pallas) and 1.18 (Baranova).
- No clear sign that Pallas BC would be particularly overestimated.
- BC overestimated especially when BC concentration is low (i.e. summertime in Baranova, all year round in Pallas).
- Further investigation needed to better understand the discrepancies.

Annex 1: Data description

The new data products to be made available in NILU/EBAS, Homeless data portal or FMI Open Data:

1. BC in Finland, real-time data: https://www.ilmatieteenlaitos.fi/ilmanlaatu
2. Ice Cape Base Baranova, Russia, BC data 2015-2020
3. Pallas BC data from COSMOS (2019-2020)
4. Pallas BC data from 4λ-PAAS (2019-2020)

References

Asmi, E., Backman, J., Servomaa, H., Virkkula, A., Gini, M. I., Eleftheriadis, K., Müller, T., Ohata, S., Kondo, Y., and Hyvärinen, A.: Absorption instruments inter-comparison campaign at the Arctic Pallas station, Atmos. Meas. Tech., 14, 5397–5413, https://doi.org/10.5194/amt-14-5397-2021, 2021.

EU-funded Action on Black Carbon in the Arctic, 2019. Review of observation capacities and data availability for Black Carbon in the Arctic region: EU Action on Black Carbon in the Arctic - Technical Report 1. December 2019. iv + 35pp.

Evangeliou, N., Thompson, R. L., Eckhardt, S., and Stohl, A.: Top-down estimates of black carbon emissions at high latitudes using an atmospheric transport model and a Bayesian inversion framework, Atmos. Chem. Phys., 18, 15307–15327, https://doi.org/10.5194/acp-18-15307-2018, 2018.

Eckhardt, S., Quennehen, B., Olivié, D. J. L., Berntsen, T. K., Cherian, R., Christensen, J. H., Collins, W., Crepinsek, S., Daskalakis, N., Flanner, M., Herber, A., Heyes, C., Hodnebrog, Ø., Huang, L., Kanakidou, M., Klimont, Z., Langner, J., Law, K. S., Lund, M. T., Mahmood, R., Massling, A., Myriokefalitakis, S., Nielsen, I. E., Nøjgaard, J. K., Quaas, J., Quinn, P. K., Raut, J.-C., Rumbold, S. T., Schulz, M., Sharma, S., Skeie, R. B., Skov, H., Uttal, T., von Salzen, K., and Stohl, A.: Current model capabilities for simulating black carbon and sulfate concentrations in the Arctic atmosphere: a multi-model evaluation using a comprehensive measurement data set, Atmos. Chem. Phys., 15, 9413–9433, https://doi.org/10.5194/acp-15-9413-2015, 2015.

Giglio, L., Randerson, J. T., and van der Werf, G. R., (2013), Analysis of daily, monthly, and annual burned area using the fourth-generation global fire emissions database (GFED4) J. Geophys. Res. Biogeosci., 118, 317–328, doi:10.1002/jgrg.20042.

Grythe, H., Kristiansen, N. I., Groot Zwaaftink, C. D., Eckhardt, S., Ström, J., Tunved, P., Krejci, R., and Stohl, A.: A new aerosol wet removal scheme for the Lagrangian particle model FLEXPART v10, Geosci. Model Dev., 10, 1447–1466, https://doi.org/10.5194/gmd-10-1447-2017, 2017.

Hyvärinen, A.-P., Kolmonen, P., Kerminen, V.-M., Virkkula, A., Leskinen, A., Komppula, M., Hatakka, J., Burkhart, J., Stohl, A., Aalto, P., Kulmala, M., Lehtinen, K.E.J., Viisanen, Y. and Lihavainen, H., Aerosol black carbon at five background measurement sites over Finland, a gateway to the Arctic, Atmospheric Environment, 45(24), 4042-4050, doi:10.1016/j.atmosenv.2011.04.026, 2011.

Klimont, Z., Kupiainen, K., Heyes, C., Purohit, P., Cofala, J., Rafaj, P., Borken-Kleefeld, J., and Schöpp, W.: Global anthropogenic emissions of particulate matter including black carbon, Atmos. Chem. Phys., 17, 8681–8723, https://doi.org/10.5194/acp-17-8681-2017, 2017.

Pisso, I., Sollum, E., Grythe, H., Kristiansen, N. I., Cassiani, M., Eckhardt, S., Arnold, D., Morton, D., Thompson, R. L., Groot Zwaaftink, C. D., Evangeliou, N., Sodemann, H., Haimberger, L., Henne, S., Brunner, D., Burkhart, J. F., Fouilloux, A., Brioude, J., Philipp, A., Seibert, P., and Stohl, A.: The Lagrangian particle dispersion model FLEXPART version 10.4, Geosci. Model Dev., 12, 4955–4997, https://doi.org/10.5194/gmd-12-4955-2019, 2019.

Schmale, J., Sharma, S., Decesari, S., Pernov, J., Massling, A., Hansson, H.-C., von Salzen, K., Skov, H., Andrews, E., Quinn, P. K., Upchurch, L. M., Eleftheriadis, K., Traversi, R., Gilardoni, S., Mazzola, M., Laing, J., and Hopke, P.: Pan-Arctic seasonal cycles and long-term trends of aerosol properties from 10 observatories, Atmos. Chem. Phys., 22, 3067–3096, https://doi.org/10.5194/acp-22-3067-2022, 2022.

Funded by the
European Union

ABC iCAP
Arctic Black Carbon